

## Inhibition Mode of a Bisubstrate Inhibitor of KDO8P Synthase: A Frequency-Selective REDOR Solid-State and Solution NMR Characterization

Lilia Kaustov,<sup>†</sup> Shifi Kababya,<sup>†</sup> Valery Belakhov,<sup>†</sup> Timor Baasov,<sup>\*,†</sup>  
Yuval Shoham,<sup>‡</sup> and Asher Schmidt<sup>\*,†</sup>

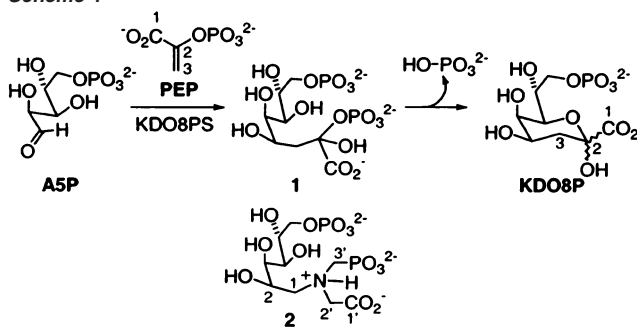
*Department of Chemistry and Institute of Catalysis Science and Technology, and Department of Food Engineering & Biotechnology, Technion-Israel Institute of Technology, Haifa 32000, Israel*

Received September 25, 2002; E-mail: chrschm@tx.technion.ac.il; chtimor@tx.technion.ac.il

**Abstract:** In this report the mode of inhibition of mechanism-based inhibitor (**2**,  $K_i = 0.4 \mu\text{M}$ ) of 3-deoxy-D-manno-2-octulosonate-8-phosphate synthase (KDO8PS), which was designed to mimic the combined key features of its natural substrates arabinose-5-phosphate (A5P) and phosphoenolpyruvate (PEP) into a single molecule, was investigated. Our earlier solid-state NMR observations identified the inhibitor to bind in a way that partly mimics A5P, while the phosphonate moiety of its PEP-mimicking part exhibits no interactions with enzyme residues. This result was apparently in disagreement with the competitive inhibition of **2** against PEP and with the later solved crystal structure of KDO8PS–**2** binary complex identifying the interactions of its PEP-mimicking part with the enzyme residues that were not detected by solid-state NMR. To solve this discrepancy, further solid-state REDOR NMR and <sup>31</sup>P solution NMR experiments were applied to a variety of enzyme complexes with the substrates and inhibitor. In particular, a novel frequency-selective REDOR experiment was developed and applied. Integration of the solution and solid-state NMR data clearly demonstrates that under conditions of stoichiometric enzyme–ligand ratio at thermodynamic equilibrium (a) PEP binding is unperturbed by the presence of **2** and (b) both PEP and **2** can bind simultaneously to the synthase, i.e., form a ternary complex with PEP occupying its own subsite and **2** occupying A5P's subsite. The latter observation suggests that under the conditions used in our NMR measurements, the inhibition pattern of **2** against PEP should have a mixed type character. Furthermore, the NMR data directly demonstrate the distinction between the relative binding strength of the two moieties of **2**: enzyme interactions with PEP-mimicking moiety are much weaker than those with the A5P moiety. This observation is in agreement with KDO8PS–**2** crystal structure showing only remote contacts of the phosphonate due to large structural changes of binding site residues. It is concluded that these phosphonate–enzyme interactions evidenced by both <sup>31</sup>P solution NMR and X-ray are too weak to be preserved under the lyophilization of KDO8PS–**2** binary complex and therefore are not evidenced by the solid-state REDOR spectra.

The enzyme 3-deoxy-D-manno-2-octulosonate-8-phosphate (KDO8P) synthase (KDO8PS) (EC 4.1.2.16) catalyzes the condensation reaction between D-arabinose-5-phosphate (A5P) and phosphoenolpyruvate (PEP) to form KDO8P and inorganic phosphate<sup>1</sup> (Scheme 1). This important enzymatic reaction controls the carbon flow in the biosynthetic formation of an unusual eight-carbon sugar 3-deoxy-D-manno-2-octulosonate (KDO). This enzymatic reaction plays a crucial role in the assembly process of the lipopolysaccharides of most Gram-negative bacteria and is therefore an attractive target for the design of novel antibacterial drugs.<sup>2,3</sup>

**Scheme 1**



The mechanism of action of KDO8PS has been studied extensively. Steady-state inhibition kinetics suggested that catalysis proceeds via a sequentially ordered Bi–Bi mechanism in which the enzyme binds PEP prior to the binding of A5P and releases KDO8P only after dissociation of Pi.<sup>4</sup> However, pre-steady-state kinetics under single-turnover conditions showed

<sup>†</sup> Department of Chemistry and Institute of Catalysis Science and Technology.

<sup>‡</sup> Department of Food Engineering & Biotechnology.

(1) Ray, P. H. *J. Bacteriol.* **1980**, *141*, 635–644.

(2) Anderson, L., Unger, F. M., Eds. *Bacterial Lipopolysaccharides*, ACS Symp Series 231; American Chemical Society: Washington, DC, 1983.

(3) Inouye, M. In *Bacterial Outer Membrane: Biogenesis and Function*; Wiley: New York, 1979.

that the synthase can bind either A5P or PEP first.<sup>5</sup> Applying solid-state rotational-echo double-resonance (REDOR) NMR to binary complexes of the synthase with each of its natural substrates, PEP and A5P, the first direct identification of active site residues of KDO8PS was made, showing two different, independent sets of enzyme residues that bind the phosphate groups of each substrate,<sup>6,7</sup> in accordance with the pre-steady-state kinetic studies mentioned above. In parallel, the first X-ray crystal structure of KDO8PS was determined, mapping the adjacent subsites occupied by sulfate ions replacing the natural substrates.<sup>8,9</sup> Subsequently, Kretsinger and co-workers used molecular replacement to solve another structure of KDO8PS in the presence of both substrates, PEP and A5P. However, neither enzyme-bound substrates nor the bound products could be identified.<sup>10</sup>

On the basis of the active site architecture of KDO8PS and substrate modeling, it was suggested that the catalytic reaction proceeds via acyclic intermediate **1** (Scheme 1), with A5P maintained in an open stretched form before it reacts with PEP. This conclusion is in agreement with earlier studies where the first acyclic bisubstrate inhibitor (**2**) of KDO8PS was synthesized and characterized ( $K_i = 0.4 \mu\text{M}$ ), whose high potency supported a mechanism involving formation of the acyclic bisphosphate intermediate **1** (Scheme 1).<sup>11</sup> This analog was designed to mimic the putative acyclic intermediate **1** by combining the key features of A5P and PEP into a single molecule, with the glyphosate moiety assuming the role of PEP. Indeed, this mechanism-based bisubstrate inhibitor was also found to be competitive against PEP.<sup>11</sup> However, our solid-state NMR investigation clearly showed that in the lyophilized KDO8PS–**2** binary complex binding of **2** resembles that of A5P alone, while no interactions of the phosphonate moiety could be detected. On the basis of these results, it was suggested that **2** is best characterized as a A5P-based inhibitor.<sup>7</sup> This conclusion, based on the NMR measurements, is apparently in disagreement with the competitive inhibition of **2** against PEP. In addition, the recently solved crystal structure of KDO8PS–**2** complex<sup>12</sup> identified interactions between the phosphonate moiety with enzyme residues that were not detected by solid-state NMR.

Resolving the discrepancy between the kinetic and X-ray observations and our solid-state NMR measurements is the goal of this work. Whether the discrepancies originate in differences of preparation conditions of samples whose integrated insight should yield a more comprehensive description of the complex system or merely reflect methodological artifacts is important to delineate. For example, crystal growth of E–**2** complex for X-ray studies was done in the presence of a large excess of **2**,

while the NMR complex was obtained from about an equimolar solution. In the former, an attempt to produce a uniform single state of the complex is made; in the latter, an attempt to preserve a state of thermodynamic equilibrium with partial binding and conformational heterogeneities is achieved. These issues are addressed in this work by further application of both solid-state NMR and <sup>31</sup>P solution NMR experiments. In addition, a novel DANTE-based, frequency-selective REDOR NMR technique was developed and its application to the ternary E–**2**–PEP system will be described. The combination of solution and solid-state NMR establishes a refined description of the actual mode of inhibition employed by **2**. The latter clearly show the tighter binding of PEP vs **2**, and a tighter binding of **2**'s A5P part vs its PEP mimicking moiety.

## Experimental Section

**General Methods.** The potassium salt of PEP was prepared in large quantities as already described.<sup>13</sup> All other chemicals used in this study were purchased from Aldrich or from Sigma and were used without further purification. The labeled **2**'s, [2-<sup>13</sup>C]**2** and [1'-<sup>13</sup>C]**2** were prepared by using a recently developed one-step procedure.<sup>11</sup> This procedure employs the direct reductive amination in aqueous media between [2-<sup>13</sup>C]-D-mannose-6-phosphate and glyphosate [*N*-(phosphonomethyl)glycine, Glp] to provide [2-<sup>13</sup>C]**2** in one step. [2-<sup>13</sup>C]-D-Mannose-6-phosphate was prepared by enzymatic phosphorylation of [2-<sup>13</sup>C]-mannose [96% <sup>13</sup>C, Cambridge Isotope Laboratories (CIL)].<sup>13</sup> Using D-mannose-6-phosphate and [1-<sup>13</sup>C]-Glp (the generous gift of Prof. J. Schaefer, Washington University, St. Louis, MO), we prepared [1'-<sup>13</sup>C]**2**. The labeled [2-<sup>13</sup>C]**2** and [1'-<sup>13</sup>C]**2** were isolated in yields [after ion-exchange chromatography on AG 1 × 8 (100–200 mesh, HCO<sub>3</sub><sup>-</sup> form), eluted with a linear gradient (0–0.6 M) of triethylammonium bicarbonate buffer (pH 7.5), followed by passage through a column Dowex 50W (K<sup>+</sup> form)] of 56 and 53%, respectively, as potassium salts.

**Solution NMR Data.** [2-<sup>13</sup>C]**2** (K<sup>+</sup> salt): <sup>13</sup>C NMR (D<sub>2</sub>O, pD = 11.0, 100 MHz)  $\delta$  67.3; <sup>31</sup>P NMR (proton decoupled, D<sub>2</sub>O, 81.0 MHz) pD = 7.3  $\delta$  5.0 (CH<sub>2</sub>OP), 6.6 (CH<sub>2</sub>P), pD = 11.0  $\delta$  5.4 (CH<sub>2</sub>OP), 16.9 (CH<sub>2</sub>P). [2-<sup>13</sup>C]-D-Mannose-6-phosphate (K<sup>+</sup> salt): <sup>13</sup>C NMR (D<sub>2</sub>O, pD = 6.6, 100 MHz)  $\delta$  73.3, 73.9; <sup>31</sup>P NMR (proton decoupled, D<sub>2</sub>O, 81.0 MHz) pD = 6.6  $\delta$  4.01 (CH<sub>2</sub>OP).

**Overexpression and Purification of KDO8PS.** KDO8PS and [*u*-<sup>15</sup>N]KDO8PS (specific catalytic activity 9 units/mg) was isolated from the overproducing *Escherichia coli* DH5 $\alpha$  (pJU1) strain, as previously described.<sup>4</sup> The recombinant enzyme and its labeled variant was purified according to the method previously reported by Ray<sup>1</sup> with slight modifications.<sup>4</sup> All manipulations were carried out at 4 °C. All buffers used during the purification contained 0.1 mM dithiothreitol (DTT); the pH of the buffers was determined at 10 °C.

**Enzyme Activity Assay.** Unless otherwise stated, the enzyme activity was assayed in 1.0 mL of a reaction buffer consisting of 0.1 M Tris/HCl, pH 7.3, 0.2 mM PEP, and 0.5 mM A5P. Following equilibration at 37 °C for 2 min, KDO8PS (10  $\mu\text{L}$ , at a final concentration of approximately 30 nM) was added, and the decrease in the absorbance difference between 232 and 350 nm (as internal reference) was monitored as a function of time (MS-DOS UV/VIS software). This method<sup>14</sup> is based on the absorbance difference at 232 nm between PEP ( $\epsilon = 2840 \text{ M}^{-1} \text{ cm}^{-1}$ ) and the other substrates and products ( $\epsilon < 60 \text{ M}^{-1} \text{ cm}^{-1}$ ) under the assay conditions. The initial rate was calculated from a linear least-squares fit to the first 30 s of the progress curve. One unit of the enzyme activity is defined as the amount that catalyzes the consumption of 1  $\mu\text{mol}$  PEP per min at 37

- (4) Kohen, A.; Jakob, A.; Baasov, T. *Eur. J. Biochem.* **1992**, *208*, 443–449.
- (5) Liang, P.; Lewis, J.; Anderson, K. S.; Kohen, A.; D'Souza, W. F.; Benenson, Y.; Baasov, T. *Biochemistry* **1998**, *37*, 16390–16399.
- (6) Kaustov, L.; Kababya, S.; Du, S.; Baasov, T.; Grooper, S.; Shoham, Y.; Schmidt, A. *J. Am. Chem. Soc.* **2000**, *122*, 2649–2650.
- (7) Kaustov, L.; Kababya, S.; Du, S.; Baasov, T.; Grooper, S.; Shoham, Y.; Schmidt, A. *Biochemistry* **2000**, *39*, 14865–14876.
- (8) Radaev, S.; Dastidar, P.; Patel, M.; Woodard, R. W.; Gatti, D. L. *J. Biol. Chem.* **2000**, *275*, 9476–9484.
- (9) Radaev, S.; Dastidar, P.; Patel, M.; Woodard, R. W.; Gatti, D. L. *Acta Crystallogr.* **2000**, *D56*, 516–519.
- (10) Wagner, T.; Kretsinger, R. H.; Bauerle, R.; Tolbert, W. D. *J. Mol. Biol.* **2000**, *301*, 233–238.
- (11) Du, S.; Faiger, H.; Belakhov, V.; Baasov, T. *Bioorg. Med. Chem.* **1999**, *7*, 2671–2682.
- (12) Asojo, O.; Friedman, J.; Adir, N.; Belakhov, V.; Shoham, Y.; Baasov, Y. *Biochemistry* **2001**, *40*, 6326–6334.

- (13) Hirschbein, B. L.; Mazenod, F. P.; Whitesides, G. M. *J. Org. Chem.* **1982**, *47*, 3765–3766.
- (14) Schoner, R.; Herrmann, K. M. *J. Biol. Chem.* **1976**, *251*, 5440–5447.

°C. During the purification, the enzyme activity was monitored by the thiobarbituric acid assay method as previously reported.<sup>1</sup> Protein concentration was determined using Bio-Rad protein assay with bovine serum albumine as a standard. The enzyme concentration was determined according to the subunit molecular mass of 30 kDa (i.e., 1 mM enzyme is 30.0 mg/mL). Spectrophotometric measurements were made on a Hewlett-Packard 8452A diode array spectrophotometer using 1-cm path-length cells with a thermostated cell holder and a circulating water bath at the desired temperature.

**Preparation of Apo-enzyme and Enzyme Complexes for NMR Measurements.** (a) **Solution NMR samples.** Purified KDO8PS (typically 70–80 mg protein) was exchanged into a buffer by extensive dialysis (24 h, with 4–6 buffer replacements), containing 100 mM Tris/HCl, pH 7.3, 0.1 mM DTT and then followed by exchange of buffer to 100 mM Tris/HCl in D<sub>2</sub>O, pD 7.3. The enzyme solution was concentrated by ultrafiltration through a centricon (10 kDa cutoff) to final concentrations of 4.6–5.3 mM in the same buffer. KDO8PS complexes were prepared by direct addition of appropriate quantities of PEP and [2-<sup>13</sup>C]2 to the above enzyme solution in deuterated buffer.

(b) **Solid-State NMR Samples.** Purified KDO8PS was exchanged into a buffer by extensive dialysis, 16–24 h, with 4–6 buffer replacements, containing 120 mM Mops, pH 7.3, 0.1 mM DTT and then concentrated by ultrafiltration through a centricon (10 kDa cutoff) to 150 μM. KDO8PS complexes were prepared by direct addition of appropriate quantities of PEP and [2-<sup>13</sup>C]2 to the above enzyme solution. The final solution prior to lyophilization contained 150 μM KDO8PS, 0.4% PEG (poly(ethylene glycol)-8000), 8 mM sucrose, 3.8 mM MOPS, and 0.1 mM DTT. This solution was divided into 8–10 mL aliquots, and each aliquot was placed in 250 mL flask. The aliquots were rapidly frozen in liquid nitrogen and lyophilized. Samples were completely freeze-dried within 16 h.

**NMR Spectroscopy.** (a) **Solution NMR.** Proton-decoupled <sup>31</sup>P NMR spectra with single-pulse excitation were recorded on a Bruker AM-200 at 81.0 MHz. Chemical shifts are reported (in ppm) relative to external orthophosphoric acid ( $\delta = 0.0$ ) in D<sub>2</sub>O. All experiments were performed at 6 °C, using 5-mm high-resolution NMR tubes. Spectra were acquired with 2 s repetition delay, except for measurements of the spectra in Figures 6c and 6d for which 9 s repetition delay was used. Data acquisition times of the enzyme complexes were between 3 and 7 h.

(b) **Solid-State NMR.** NMR measurements were carried out on a Chemagnetics/Varian 300 MHz CMX-*infinity* solid-state NMR spectrometer equipped with 3 rf channels and a triple resonance probe using 5 mm zirconia rotors. Samples were spun at 5000 ± 2 Hz and were maintained at 1 ± 0.1 °C as a precaution throughout the experiments. Cross polarization magic angle spinning (CPMAS) echo experiments were acquired with a 5 μs <sup>1</sup>H-90°, 10 μs X-180° pulse widths, 100 kHz <sup>1</sup>H decoupling, and 2 s repetition delay; Hartmann–Hahn rf levels were matched at 50 kHz, with 0.7, 2, and 2 ms contact times for <sup>15</sup>N, <sup>13</sup>C, and <sup>31</sup>P, respectively. The chemical shifts of <sup>15</sup>N, <sup>13</sup>C, and <sup>31</sup>P are reported relative to solid (<sup>15</sup>NH<sub>4</sub>)<sub>2</sub>SO<sub>4</sub>, TMS, and 85% H<sub>3</sub>PO<sub>4</sub>, respectively, with accuracy of ±0.3 ppm. REDOR data was acquired using a REDOR pulse sequence with refocusing  $\pi$  pulses on each rotor period ( $T_R$ ) on the observe channel, and dephasing  $\pi$  pulses in the middle of each rotor period on the nonobserved nuclei, followed by additional two rotor periods with chemical shift echo pulse in the middle. The REDOR pulses on both channels followed the xy-8 phase cycling scheme<sup>15</sup> in order to minimize chemical shift offset errors. REDOR data acquired with dephasing pulses are denoted *S*, while data without dephasing pulses serve for a reference and are denoted *S*<sub>0</sub>. Difference data obtained by the subtraction *S*<sub>0</sub> – *S* are denoted  $\Delta S$ , and yield spectra which exhibit peaks of dipolar coupled chemical species exclusively. Cross polarization excitation was employed in all

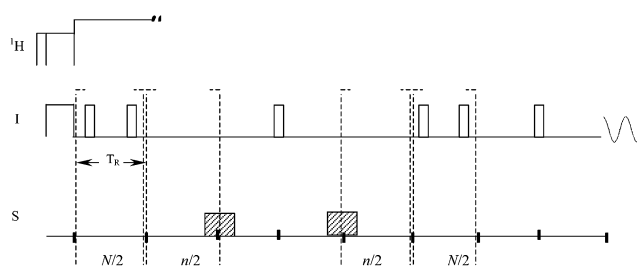


**Figure 1.** DANTE-based frequency-selective REDOR (dbFSR) pulse sequence. Recoupling pulses are applied to the observed *I* nuclei at 1/4 and 3/4  $T_R$ , symmetric with respect to a central  $\pi$ -refocusing pulse ( $N/2 T_R$  on each side). Additional *I*  $\pi$  pulse within a  $2T_R$  period is appended to form a chemical shift echo. Frequency-selective recoupling of *I* and *S* spin pairs is achieved by the application of two DANTE  $\pi/2$  pulses to the *S* nuclei, symmetric with respect to a central  $\pi$ -refocusing *I* pulse. Each DANTE  $\pi/2$  pulse is composed of  $n/2$  rotor-synchronized  $\pi/n$  RF pulses. Reference, full echo signal (*S*<sub>0</sub>), is obtained with *I* pulses only; frequency-selective recoupled signal (*S*) is obtained by application of the DANTE pulses.

REDOR experiments using the parameters described above. Up to 80 000 scans were collected depending on sample weight and on the desired S/N ratio. Sample weights ranged between 130 and 200 mg, with enzyme weight being about 40%.

(c) **DANTE-Based, Frequency-Selective REDOR.** A DANTE-based, frequency-selective REDOR (dbFSR) experiment enable, within a class of nuclei (e.g., <sup>13</sup>C), the selective recoupling of only chemical moieties within a narrow frequency (chemical shift) range. In this experiment we combine the REDOR pulse sequence with the DANTE<sup>16</sup> inversion in order to reintroduce the dipolar interaction between the observed nuclei (*I*) and certain chemical moieties within a narrow frequency range of the nonobserved nuclei (*S*). The frequency selectivity is achieved by applying to the nonobserved nuclei two DANTE  $\pi/2$  pulses (rotor synchronized) that involve  $n/2$ ,  $\pi/n$  rf pulses each, interleaved with an interval of one rotor period. The pulse sequence is shown in Figure 1. In the absence of DANTE recoupling pulses, this scheme yields a full, *I* nuclei, reference spectrum identical to the nonselective REDOR. Its difference spectrum,  $\Delta S$ , however, exhibits peaks of *I* nuclei due to dipolar coupling with *S* nuclei within a narrow chemical shift range only. This approach therefore enables us to identify in the difference spectrum all interacting *I* species in a single experiment. It should be noted that frequency-selective recoupling schemes were introduced before by Schaefer and co-workers,<sup>17</sup> employing DANTE  $\pi$ -pulses replacing all dephasing pulses, and more recently by Griffin and co-workers,<sup>18</sup> employing soft Gaussian  $\pi$ -pulses (applied both to *I* and *S*). A full account of our new pulse sequence and its scope of application will be given elsewhere.

Experimental parameters used in this work were 5000 Hz spinning speed, eight (*n*) 5.0 μs DANTE pulses with rf power of  $\nu_1 = 12.5$  kHz separated by one rotor period (200.0 μs). All other parameters are as described above for the REDOR experiment.

**Abbreviations:** A5P, D-arabinose-5-phosphate; PEP, phosphoenolpyruvate; KDO8P, 3-deoxy-D-manno-2-octulosonate-8-phosphate; KDO8PS, 3-deoxy-D-manno-2-octulosonate-8-phosphate synthase; REDOR, rotational-echo double-resonance; dbFSR, DANTE-based frequency-selective REDOR.

## Results and Discussion

Our earlier NMR observations identified the bisubstrate inhibitor (**2**) to bind in a way that partly mimics A5P, while

- (16) Freeman, R.; Morris, G. A. *J. Magn. Reson.* **1978**, *29*, 433–462.  
 (17) Klug, C. A.; Zhu, W.; Tasaki, K.; Schaefer, J. *Macromolecules* **1997**, *30*, 1734–1740.  
 (18) Jaroniec, C. P.; Tounge, B. A.; Herzfeld, J.; Griffin, R. G. *J. Am. Chem. Soc.* **2001**, *123*, 3507–3519.

(15) Gullion, T. G.; Baker, D. B.; Conradi, M. S. *J. Magn. Reson.* **1990**, *89*, 479–484.

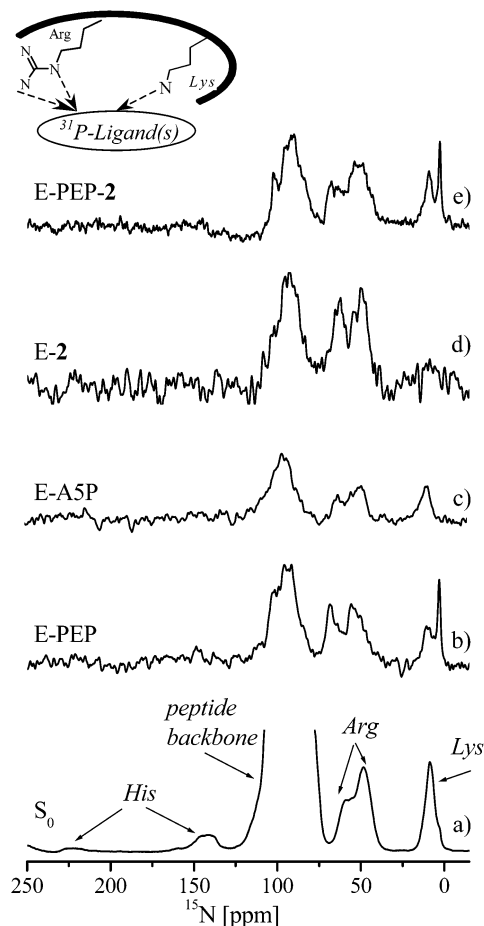


**Figure 2.**  $64T_R$   $^{15}\text{N}\{^{31}\text{P}\}$  REDOR spectra of enzyme complexes: (a) reference,  $S_0$ , and (b) difference  $\Delta S$ , of the  $[\text{U-}^{15}\text{N}]\text{KDO8PS}-[1\text{-}^{13}\text{C}]\text{PEP}$ ,  $\Delta S$ , 1:1 molar ratio; (c)  $[\text{U-}^{15}\text{N}]\text{KDO8PS}-[1\text{-}^{13}\text{C}]\text{A5P}$ ,  $\Delta S$  1:1 molar ratio; (d)  $[\text{U-}^{15}\text{N}]\text{KDO8PS}-\mathbf{2}$ ,  $\Delta S$ , 1:1 molar ratio; (e)  $[\text{U-}^{15}\text{N}]\text{KDO8PS}-\text{PEP}-\mathbf{2}$ , 1:1.2:1.2 molar ratio. Spectrum b is vertically expanded by a factor of 25 relative to its reference spectrum (a). Spectra (c), (d), and (e) are expanded by the same factor relative to their respective reference spectra (not shown). The intact lysine spectral fingerprint of PEP binding is clearly shown in spectrum (e) along with the composed arginine difference, suggesting that PEP's binding is not perturbed by  $\mathbf{2}$ . The inset illustrates the monitored intermolecular  $^{15}\text{N}-^{31}\text{P}$  interactions.

the phosphonate moiety of its PEP-mimicking part exhibits no interactions with enzyme residues. In view of  $\mathbf{2}$ 's low  $K_i$  ( $0.4 \mu\text{M}$ ) compared with the  $K_m$  of PEP ( $6.0 \mu\text{M}$ ), and its competitive inhibition against PEP, the first question addressed is whether  $\mathbf{2}$  would block PEP binding in the ternary system. For this purpose, the ternary system KDO8PS- $\mathbf{2}$ -PEP with a 1:1.2:1.2 molar ratio was prepared and subjected to both solid-state and  $^{31}\text{P}$  solution NMR characterization.

**Comparison of Enzyme-Ligand Interactions in Binary Complexes vs E- $\mathbf{2}$ -PEP by  $^{15}\text{N}\{^{31}\text{P}\}$  REDOR NMR.** The  $64 T_R$   $^{15}\text{N}\{^{31}\text{P}\}$  REDOR reference spectrum of the ternary system E- $\mathbf{2}$ -PEP is shown in Figure 2a, in which the peptide backbone gives rise to an intense 95 ppm peak (truncated). Additional resolved peaks in this spectrum are attributed to the nitrogen atoms of side chain histidine (nonprotonated,  $\delta_1$ , 224 ppm; protonated,  $\epsilon_2$ , 143 ppm), guanidino arginine (internal  $\epsilon$ , 60 ppm; external  $\eta$ , 49 ppm), and side chain lysine ( $\epsilon$ , 9 ppm).<sup>7,19</sup> In our previous solid-state NMR studies of the enzyme binary

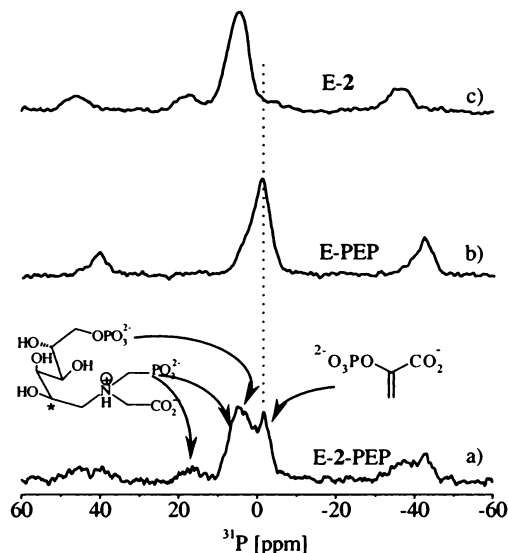


**Figure 3.**  $^{31}\text{P}$  CPMAS NMR spectra of enzyme complexes: (a)  $[\text{U-}^{15}\text{N}]\text{KDO8PS}-[2\text{-}^{13}\text{C}]\mathbf{2}$ -PEP; (b)  $[\text{U-}^{15}\text{N}]\text{KDO8PS}$ -PEP; (c)  $[\text{U-}^{15}\text{N}]\text{KDO8PS}-\mathbf{2}$ . Spinning sidebands are denoted ss. Three complexes are with equimolar ratios.

complexes with PEP, A5P and  $\mathbf{2}$ ,  $\{^{15}\text{N}\}^{31}\text{P}$  REDOR experiments yielded  $^{15}\text{N}$  REDOR difference spectra of enzyme residues, exclusively responsible for recognition and binding of each of the three ligands.<sup>7</sup> Their respective REDOR difference spectra are reproduced<sup>7</sup> in Figures 2b-d, respectively. Specifically, basic residues that bind the negatively charged phosphate and phosphonate moieties were probed. For PEP and A5P, two different sets of enzyme lysine and arginine residues with different spectral (chemical) characteristics were observed: narrow peaks with substantially modified isotropic chemical shifts for those that bind PEP (Figure 2b) and broad peaks with generic chemical shifts for those that bind A5P (Figure 2c). Only arginine residues represented by broad peaks at generic chemical shifts were identified in the spectrum of the E- $\mathbf{2}$  complex (Figure 2d), partially resembling those of the E-A5P complex. In anticipation of the bisubstrate inhibitor to interfere with PEP's binding, the typical spectral signature of enzyme residues that bind PEP (as shown in Figure 2b) should therefore not appear in the  $^{15}\text{N}\{^{31}\text{P}\}$  REDOR difference spectrum of the ternary KDO8PS- $\mathbf{2}$ -PEP system. However, its  $64T_R$   $^{15}\text{N}\{^{31}\text{P}\}$  REDOR difference spectrum shown in Figure 2e exhibits the spectral fingerprint that was identified as PEP's binding lysine residues (9.0 and 3.0 ppm peaks). In addition, a backbone nitrogen peak is observed (95 ppm) as well as a complex peak of arginine residues visualized as a superposition of contributions of those that bind PEP as in spectrum 2b (E-PEP) and a relatively smaller contribution from the arginines that bind  $\mathbf{2}$  as shown in spectrum 2d (E- $\mathbf{2}$ ). Contrary to our expectation, these results indicate that the binding of PEP is not affected by the presence of  $\mathbf{2}$ . It is the inhibitor's binding which appears impeded, as is manifested by the reduction of the intensity of the arginine difference peak in Figure 2e relative to that in 2d.

**$^{31}\text{P}$  CPMAS Characterization of E- $\mathbf{2}$ -PEP.** In preparation for frequency-selective REDOR experiments, the  $^{31}\text{P}$  CPMAS NMR spectrum of the ternary E- $\mathbf{2}$ -PEP system was recorded and is shown in Figure 3a along with the previously published spectra of E-PEP and E- $\mathbf{2}$  binary complexes<sup>7</sup> in Figures 3b and 3c, respectively. Spectrum 3a depicts three peaks: a

(19) McDowell, L. M.; Schmidt, A.; Cohen, E. R.; Studelska, D. R.; Schaefer, J. *J. Mol. Biol.* **1996**, *256*, 160-171.

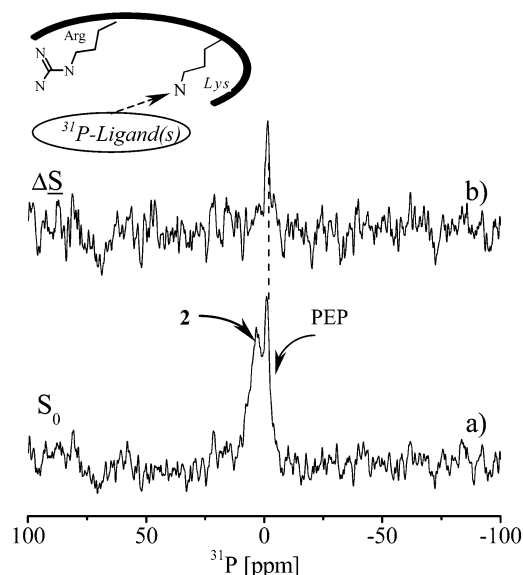


**Figure 4.**  $64T_R$   $^{31}\text{P}\{^{15}\text{N}\}$  dbFSR spectra of the ternary system  $[\text{U-}^{15}\text{N}]\text{-KDO8PS-}[\text{2-}^{13}\text{C}]\text{2-PEP}$ : (a) reference,  $S_0$ , (b) difference,  $\Delta S$ . DANTE frequency is on the 3 ppm lysine peak. The difference peak at the PEP phosphate position confirms for this ternary system that the lysine residues identified by the  $^{15}\text{N}\{^{31}\text{P}\}$  REDOR in Figure 2b bind PEP. The inset illustrates the monitored intermolecular  $^{31}\text{P-}^{15}\text{N}\{\text{Lys}\}$  interactions.

relatively narrow  $-1.5$  ppm peak of PEP phosphate, shifted upfield relative to its  $-1.0$  ppm position in the binary complex (Figure 3b); two broad peaks at the same positions as found for the binary  $\text{KDO8PS-2}$  complex<sup>7</sup> (spectrum 3c), the first, centered at  $4.4$  ppm is due to the unresolved phosphate ( $3.8$  ppm) and phosphonate ( $5.6$  ppm) moieties of **2**, and a  $16.0$  ppm phosphonate peak, representing a modified phosphonate form. The latter assignment was accomplished via REDOR experiments utilizing intramolecular (P–C) and intermolecular (P–N) dipolar interactions and is detailed in ref 7. The occurrence of an additional chemical form of the inhibitor’s glyphosate part ( $16$  ppm peak) is attributed to its weaker binding, where “chemical/structural protection” is not offered by the synthase as for tighter bound ligands.

**Identification of Lysine-Bound Moieties of E–2–PEP by  $^{31}\text{P}\{^{15}\text{N}\}$  dbFSR.** To obtain additional, independent identification for which of the phosphate and phosphonate groups of PEP and **2** interact with lysine residues of the synthase, we choose to monitor the  $^{31}\text{P}$  nuclei, where the  $^{31}\text{P}$ -bearing moieties of PEP and **2** are partially resolved (Figure 3a) and reintroduction of dipolar coupling only to lysine residues ( $^{15}\text{N}$ ) is sought. For this purpose, we devised a DANTE-based frequency-selective REDOR (dbFSR) experiment.<sup>20</sup> Here, the selective recoupling of chemical moieties only within a narrow frequency (chemical shift) range of a certain class of nuclei, e.g.,  $^{15}\text{N}$ , is facilitated. This experimental approach is advantageous since it enables arbitrary selection of the type of moieties within a uniformly  $^{15}\text{N}$ -labeled enzyme, avoiding the need to prepare specifically  $^{15}\text{N}$ -labeled enzyme samples. Applying to the dephased nuclei ( $^{15}\text{N}$ ) only frequency-selective DANTE pulses also minimizes complications that may arise due to homonuclear  $^{15}\text{N-}^{15}\text{N}$  dipolar interactions.<sup>18</sup>

The  $64T_R$   $^{31}\text{P}\{^{15}\text{N}\}$  dbFSR reference spectrum of the E–2–PEP system (1:1.2:1.2), shown in Figure 4a, depicts the two

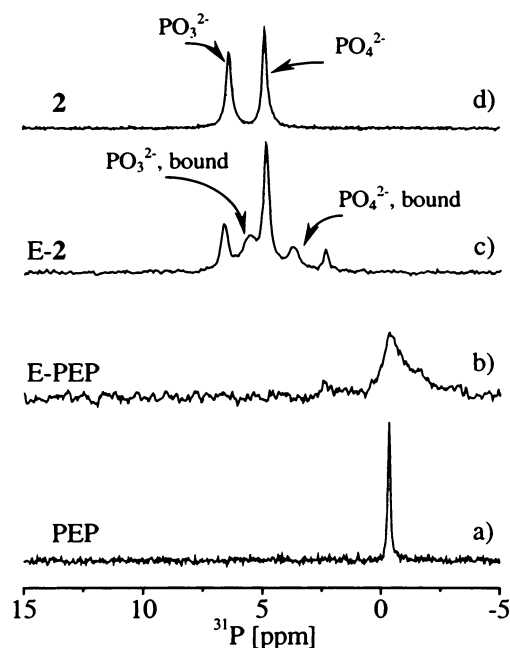


**Figure 5.**  $^{31}\text{P}$  solution NMR spectra of (a) PEP, (b)  $\text{KDO8PS-PEP}$  complex, 1:1 molar ratio; (c)  $\text{KDO8PS-2}$  complex, 1:1 molar ratio; (d) inhibitor **2**.

partially resolved  $-1.4$  and  $3.7$  ppm peaks of PEP phosphate and of the inhibitor’s phosphate and phosphonate moieties (nonresolved), respectively. The frequency-selective difference spectrum in Figure 4b shows a pronounced  $-1.5$  ppm peak only at the position of PEP’s phosphate group. This spectrum therefore confirms that in the 1:1.2:1.2 molar ratio E–2–PEP ternary system PEP binding by the synthase is unperturbed by the presence of the inhibitor. This is fully in accordance with our determination above based on the unaltered lysine fingerprint of enzyme-bound PEP seen in the  $^{15}\text{N}\{^{31}\text{P}\}$  REDOR data (Figure 2e). Since our solid-state NMR observations report on a state of thermodynamic equilibrium of the ternary E–2–PEP system prior to lyophilization, we conclude that PEP’s binding by the enzyme is stronger than that of **2**–phosphonate moiety. Hence, since phosphonate–enzyme interactions fail to compete with PEP–enzyme interactions, the origin for **2**’s potent inhibition is primarily attributed to its strong binding at the A5P site, suggesting that it should also be found highly competitive against A5P.

**$^{31}\text{P}$  Solution NMR Identification of Enzyme–Phosphorus Interactions of E–PEP and E–2.** To further complement the above solid-state NMR observations, analogous  $^{31}\text{P}$  solution NMR measurements were employed to investigate the ternary E–2–PEP system in solution under conditions of thermodynamic equilibrium. First, the  $^{31}\text{P}$  solution NMR spectra of the two binary complexes, E–PEP and E–2 with 1:1 molar ratios, are shown in Figures 5b and 5c, respectively, along with the respective reference spectra of PEP and **2** in Figures 5a and 5d (all solutions at pH 7.3). Free PEP depicts a peak at  $-0.3$  ppm (Figure 5a) that upon enzyme binding is substantially broadened and shifted to  $-0.5$  ppm (Figure 5b) and exhibits a high-field shoulder at ca.  $-1.6$  ppm. The observed line broadening results from PEP’s association to the large macromolecule and to its relayed dynamic properties.<sup>21,22</sup> The free phosphonate and phosphate moieties of **2** exhibit  $6.6$  and  $5.0$  ppm peaks, respectively (Figure 5d). Upon enzyme binding, both

(20) dbFSR technique development: Cabri, O. M.Sc. Thesis, Technion, 2002. Lipson, S. O. M.Sc. Thesis, Technion, 2003.

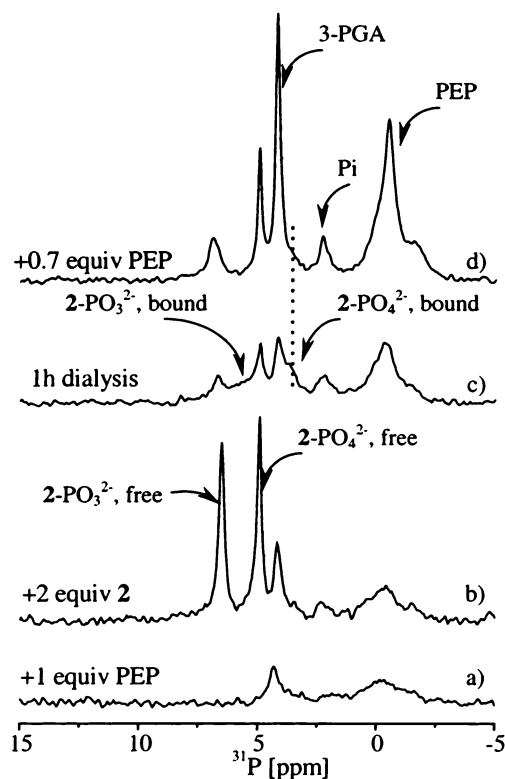


**Figure 6.**  $^{31}\text{P}$  solution NMR spectra of enzyme complexes: (a) addition of 1 equiv of PEP to apo-KDO8PS; (b) addition of 2 equiv of **2** to (a); (c) (b) after 1 h dialysis; (d) addition of 0.7 equiv of PEP to sample (c). Spectra (a) and (b) were acquired with 2 s repetition delay; spectra (b) and (c) with 9 s. Each pair of spectra is normalized separately, accounting for number of scans. Spectrum (d) shows clearly that binding of PEP to enzyme leads to release of **2**; the maintained high field 3.8 ppm shoulder of bound  $2\text{-PO}_4^{2-}$  suggests the formation of the ternary complex KDO8PS– $2\text{-PEP}$ .

peaks of the bound moieties are broadened and shifted upfield to 5.6 and 3.8 ppm, respectively, giving rise to the  $^{31}\text{P}$  spectrum in Figure 5c. This spectrum also depicts a 2.4 ppm peak due to residual inorganic phosphate, Pi. The fact that the chemical shifts of both enzyme-bound  $2\text{-phosphate}$  and  $\text{A5P-phosphate}$ <sup>22</sup> are identical, 3.8 ppm, indicates that the A5P moiety of **2** experiences a chemical environment of the synthase as that experienced by A5P, implying that **2** occupies A5P's site, in accordance with our solid-state NMR observations.<sup>7</sup>

**$^{31}\text{P}$  Solution NMR Identification of Competitive Binding of PEP and **2**.** Next, a set of  $^{31}\text{P}$  NMR measurements involving subsequent additions of both PEP and **2** were performed. The  $^{31}\text{P}$  solution NMR spectrum following the addition of 1 equiv of PEP to the apoenzyme solution shown in Figure 6a, depicts the substantially broadened peak of PEP (−0.4 ppm) (as shown in the spectrum in Figure 5a). In addition, a 4.2 ppm peak attributed to 3-PGA that is slowly formed by the conversion of PEP by residual quantities of enolase and mutase that were not fully removed during enzyme purification.<sup>23</sup> Subsequent addition of 2 equiv of **2** to the present solution gives rise to the spectrum shown in Figure 6b, exhibiting the two distinct narrow peaks of the inhibitor's unbound phosphate and phosphonate moieties at 5.0 and 6.6 ppm, respectively. Even though the peak bases

of the unbound phosphate and 3-PGA are somewhat broadened, these broadenings cannot be conclusively attributed to the bound  $^{31}\text{P}$  moieties of **2** as expected at 3.8 and 5.6 ppm (Figure 5c). It should be noted however that the −0.3 ppm peak due to PEP is slightly narrowed (Figure 6b), indicating that the binding of PEP upon addition of 2-fold excess of **2** was only slightly affected. The increase of the 4.2 ppm 3-PGA peak implies its further accumulation. This spectrum also depicts a residual 2.4 ppm Pi peak.

Subjecting the solution of Figure 6b to a 1 h dialysis (1 mL enzyme solution against 2 L buffer) gives rise to the  $^{31}\text{P}$  spectrum shown in Figure 6c, where the peak intensities of free phosphate and phosphonate of **2** are substantially reduced, implying its unbound excess was largely removed (along with 3-PGA). The unresolved broadening depicted between the peaks of the unbound **2** at 5.6 ppm, along with the broad 3.8 ppm upfield shoulder of the 4.2 ppm 3-PGA peak, are attributed to the enzyme-bound phosphonate and phosphate moieties of **2** in accordance with the chemical shifts identified for those species in the binary complex spectrum (Figure 5b). This assignment will be further substantiated below. It should be noted that in order to shorten data acquisition time, and reduce accumulation of 3-PGA, the spectra in Figures 6a,b were obtained with a repetition delay of 2 s. The spectra in Figures 6c,d were obtained with a repetition delay of 9 s, hence giving rise to the increase of the PEP and Pi peaks in 6c relative to their intensities in spectrum 6b prior to dialysis ( $T_1^{\text{PEP}} \sim 5$  s).

Addition of 0.7 equiv of PEP to the present mixture resulted not only in increased intensity of the broad PEP peak but also in a substantial intensity increase of the peaks of both free moieties of **2** (Figure 6d). This observation clearly demonstrates that PEP leads to the release of the inhibitor in accordance with our solid-state NMR data, where the stronger binding of PEP vs that of **2** was inferred. The disappearance of the broad 5.6 ppm component from spectrum 6d confirms its attribution in Figure 6c to bound phosphonate. However, the small 3.8 ppm upfield shoulder (of the intense 4.2 ppm peak of 3-PGA) indicates the presence of bound phosphate fraction of **2**, hence manifesting the tighter binding of its phosphate moiety vs that of the phosphonate. The observed partial release of **2**'s phosphate in the presence of PEP suggests that the ternary complex E– $2\text{-PEP}$  has been formed. This issue of formation of a ternary complex is further addressed and examined below.

The solution NMR observations unambiguously substantiate the notion that the binding constant of PEP is at least an order of magnitude higher than that of **2**, in full agreement with the solid-state NMR characterization. It should be pointed out that the solution NMR spectra cannot be used for a quantitative determination of bound vs free species ratio. The latter would require accurate knowledge of the NMR relaxation parameters for all species (bound and free), information that is not easy to obtain in the presence of large synthase quantities where additional processes, e.g., conversion of PEP to 3-PGA or phosphate hydrolysis, occur.<sup>24</sup>

**Identification of Formation of Ternary Complex E– $2\text{-PEP}$  by  $^{31}\text{P}\{^{13}\text{C}\}$  dbFSR NMR.** While the stronger binding of PEP vs **2** is clearly evident, the additional question that arises is whether the simultaneous binding of **2** and PEP to the synthase occurs in a ternary complex, or alternatively, is it merely two

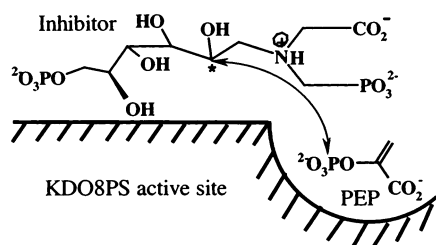
(21) Gornstein, D. G. *Phosphorus-31 NMR. Principles and Applications*; Academic Press, Inc.: London, 1984.

(22) Kaustov, L.; Baasov, T.; Schmidt, A. Submitted for publication.

(23) Zchut, R. M.Sc. Thesis, Technion, 1994.

(24) Kaustov, L. Ph.D. Thesis, Technion, 2001.

Scheme 2



separate populations of the two binary complexes, KDO8PS–2 and KDO8PS–PEP. Such a distinction is important, since it embeds information on whether the binding of PEP and that of **2** are mutually exclusive, as is implied by the kinetic characterization of **2** as a competitive inhibitor against PEP, or whether only the binding of PEP and the phosphonate of **2** are mutually exclusive. The latter possibility is visualized as the binding of **2**–phosphate in A5P's subsite together with PEP in its adjacent subsite, in a ternary complex. While the above solid-state and solution NMR data of the ternary system with the molar ratios employed suggest that a ternary complex is formed, direct experimental evidence showing molecular proximity between the inhibitor and PEP will delineate conclusively between the two possibilities.

Therefore, we have prepared the ternary system [U-<sup>15</sup>N]-KDO8PS–[2-<sup>13</sup>C]**2**–PEP, where the intermolecular dipolar interaction between PEP–phosphate and 2-<sup>13</sup>C of [2-<sup>13</sup>C]**2** was targeted as illustrated in Scheme 2. Specifically, the dbFSR experiment, monitoring the <sup>31</sup>P nuclei and recoupling them selectively to the specific <sup>13</sup>C label, was employed. Here, a frequency-selective REDOR experiment is advantageous for <sup>13</sup>C recoupling, since by selecting a small range of chemical shifts we avoid the severe complication arising otherwise from natural abundance background dephasing.<sup>25,26</sup>

Applying the 64T<sub>R</sub> <sup>31</sup>P{<sup>13</sup>C} dbFSR experiment to E–[2-<sup>13</sup>C]**2**–PEP with the frequency-selective recoupling at the predetermined <sup>13</sup>C frequency of [2-<sup>13</sup>C]**2** yields the reference and difference spectra shown in Figures 7a and 7b, respectively. The reference spectrum (Figure 7a) depicts primarily the phosphate peaks of **2** and PEP at 3.7 and –1.4 ppm, respectively, similar to the spectra in Figures 3a and 4a. The difference spectrum (Figure 7b) exhibits two peaks: a broad, major 3.8 ppm peak of <sup>31</sup>P-phosphate of **2**, exposed by the relatively strong intramolecular P–C interactions, and a smaller, sharper peak at –2.0 ppm of PEP–phosphate. The latter may arise only due to intermolecular dipolar interaction with [2-<sup>13</sup>C]**2**, hence confirming the occurrence of the ternary complex. In view of the limited signal-to-noise obtained in this difference spectrum, two additional control experiments were performed to validate the above observation. First, the <sup>13</sup>C recoupling frequency was shifted 2.5 kHz upfield (ca. 33 ppm), to a null recoupling condition with respect to the labeled carbon. The resulting 64T<sub>R</sub> <sup>31</sup>P{<sup>13</sup>C} dbFSR difference spectrum shown in Figure 7c exhibits a null difference. Second, as an additional control experiment, an identical selective recoupling experiment as used for 7a,b was applied to the [U-<sup>15</sup>N]KDO8PS–[1'-<sup>13</sup>C]**2**–PEP complex. Here, the selective recoupling frequency (at 67.5 ppm) is 7.8

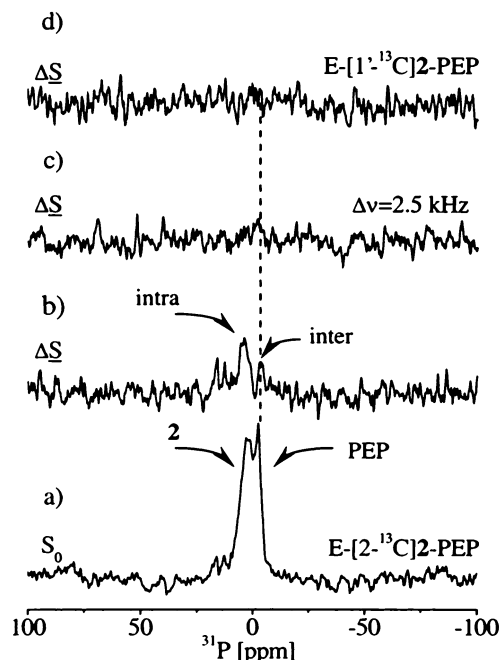


**Figure 7.** 64T<sub>R</sub> <sup>31</sup>P{<sup>13</sup>C} dbFSR spectra of [U-<sup>15</sup>N]KDO8PS–[2-<sup>13</sup>C]**2**–PEP 1:1.2:1.2 ternary complex: (a) reference, S<sub>0</sub>; (b) difference, ΔS (× 1.5); (c) difference, ΔS with DANTE irradiation frequency shifted 33 ppm downfield (+2.5 kHz positions 2-<sup>13</sup>C at a DANTE null condition); (d) 64T<sub>R</sub> <sup>31</sup>P{<sup>13</sup>C} dbFSR difference spectrum, ΔS, of [U-<sup>15</sup>N]KDO8PS–[1'-<sup>13</sup>C]**2**–PEP 1:1.2:1.2 ternary complex, with DANTE frequency as in (b); in this case the DANTE irradiation frequency is ca. –7.5 kHz off from 1'-<sup>13</sup>C, setting this carbon at a null condition. The absence of difference peaks in the two control spectra (c and d), even such arising from intramolecular interactions, validate dbFSR selectivity and the elimination of natural abundance <sup>13</sup>C background dephasing. The –2.0 ppm difference peak in (b) therefore demonstrates the intermolecular proximity of PEP-phosphate and 2-<sup>13</sup>C of **2** in the enzymes active site, indicating the formation of a ternary complex.

kHz lower than the position of the labeled 1'-<sup>13</sup>C of the inhibitor (173.0 ppm). Its null difference spectrum in Figure 7d indicates that no natural abundance <sup>13</sup>C background dephasing occurs at the selected frequency range. These experiments confirm the unambiguous identification of the small difference peak (–2.0 ppm) in 7b as a PEP phosphate peak. Therefore, the above set of frequency-selective REDOR experiments evidence the formation of the E–**2**–PEP ternary complex. At this time, the intermolecular P–C distance cannot be directly estimated from these experiments nor the fraction of **2** and PEP that is engaged in this complex. The upfield shifted difference peak at –2.0 ppm along with upfield shoulder in the solution spectra (Figure 5b, 6d) suggest that they represent enzyme-bound PEP both in the binary E–PEP and in the ternary E–**2**–PEP complexes.

## Summary and Conclusions

Our earlier solid-state REDOR NMR data showed that the enzyme binds **2** by arginine residues that interact only with its phosphate moiety in a way that partially mimics that of A5P binding.<sup>7</sup> No interactions of enzyme basic residues or of enzyme backbone with its phosphonate moiety, designed to mimic PEP, could be detected. These observations led us to suggest that the inhibitor is an A5P-based inhibitor and that its potency arises primarily from mimicking A5P. Apparently, the above conclusions were in disagreement with both the kinetic measurements that showed that **2** is competitive against PEP and also with

(25) McDowell, L. M.; Klug, C. A.; Beusen, D. D.; Schaefer, J. *Biochemistry* **1996**, *35*, 5395–5403.

(26) Garbow, J. R.; Gullion, T. In *Carbon 13 NMR Spectroscopy of Biological Systems*; Academic Press, Inc.: New York, 1995; pp 65–115.

our solution NMR results (presented here) and the X-ray crystal structure,<sup>12</sup> identifying that both the phosphate and phosphonate interact with the enzyme.

The notion based on the solid-state NMR measurements that the inhibitor is involved in much weaker interactions with the enzyme is unequivocally demonstrated by <sup>31</sup>P solution NMR under conditions of thermodynamic equilibrium: addition of a 2-fold excess of **2** to the 1:1 E-PEP complex is not sufficient to release PEP; addition of PEP to the E-**2** complex drives enzyme-bound **2** out of the binding site, with preferential release of its phosphonate moiety. Furthermore, our observations directly demonstrate the distinction between the relative binding strength of the two moieties of **2**: enzyme interactions with the PEP-mimicking moiety are weaker than those formed between the inhibitor's A5P moiety and the enzyme. It is this difference in the relative binding strength that leads to the absence of enzyme-phosphonate interactions in the solid-state NMR data: the phosphonate-enzyme interactions in the E-**2** binary complex are either not sufficiently strong to be preserved under the lyophilization transformation or they are too remote to be detected.

Moreover, both our solution and solid-state NMR observations suggest that **2** and PEP can be bound simultaneously by the synthase, i.e., form a ternary complex with PEP occupying its own subsite, and **2** occupying A5P's subsite, with its glyphosate moiety covering the PEP-filled active-site cavity. This description is visualized by the simplified model in Scheme 2. These observations clearly suggest that under conditions used in our NMR measurements, the inhibition pattern of **2** against PEP should have a mixed type character. Finally, also a careful inspection of the recently solved X-ray structure of the E-**2** binary complex<sup>12</sup> is found to be in agreement with the NMR-based distinction between the relative binding strength of the two moieties of **2**. In this structure the positions of Lys138 and Arg168, the two dominant residues in PEP-phosphate binding, undergo substantial conformational changes upon replacement of PEP with **2**: Lys138 is now pointing away from the phosphonate and Arg168 forms only a remote contact.

The integration of the understanding gained throughout this study identifying tighter binding of PEP vs **2**'s phosphonate, with the kinetic<sup>11</sup> and crystallographic<sup>12</sup> studies, leads to the conclusion that  $K_i$  is determined primarily by the phosphate binding strength of the A5P moiety of **2**. This deduced differential between the binding strength of the two moieties clearly confirms the identification of **2** as an A5P-based inhibitor and that **2** should be found competitive also against A5P. To design a more potent analog, factors that can improve the simultaneous binding strength of the phosphonate moiety will be sought.

In summary, it is shown in this work that employing advanced solid-state NMR techniques, in particular the novel frequency-selective dbFSR experiment, along with straightforward <sup>31</sup>P solution NMR, adds valuable information that is not conducive to crystallographic studies and/or kinetic characterization alone. Investigation of enzyme-ligand(s) complexes with stoichiometric compositions whose inherent heterogeneities of partial site occupancy are preserved provides an advantage for the NMR characterization, while it is a deficiency for crystallographic studies. It is the integration of the understanding gained from the different experimental approaches that comprises a more comprehensive elucidation of the nature of complex bio-macromolecular systems.

**Acknowledgment.** The authors thank Dr. Noam Adir (Chemistry, Technion) for insightful discussions and Dr. Dan Igner (Chemistry, Technion) for helpful technical support with the low-field spectrometer. This research was supported in part by the Israel Science Foundation founded by the Israel Academy of Sciences and Humanities, and by the Foundation for Promotion of Research at the Technion, A.S and T.B. (Grant 132/01), and by Technion V.P.R. Fund Rubin Scientific and Medical Fund (060-624). V.B. acknowledges the financial support by the Center of Absorption in Science, the Ministry of Immigration Absorption, and the Ministry of Science and Technology, Israel (Kamea Program).

JA028688Y